Journal of Petroleum Science and Engineering 164 (2018) 344–350

Contents lists available at ScienceDirect

Journal of Petroleum Science and Engineering

journal homepage: www.elsevier.com/locate/petrol

Numerical simulation and correction of electrical resistivity logging for different formation dip angles

Jun Zhao [a,*], Wei Li [a], Chengwen Xiao [b], Xinzhong Qi [b], Songshan Yuan [a]

[a] School of Geoscience and Technology, Southwest Petroleum University, Chengdu, Sichuan 610500, China
[b] Institute of Petroleum Exploration and Development, PetroChinaTarim Oilfield Branch, Korla, Xinjiang 841000, China

ARTICLE INFO

Keywords:
Resistivity logging
Formation dip
Formation anisotropy
Resistivity correction method
Finite-element method

ABSTRACT

Resistivity is an important parameter used to identify the properties of reservoir fluids. In an inclined stratum, the relative position of the wellbore trajectory and changes in the formation alter the response mechanism of normal well logging tools, and the response of well logging tools is different from that in an inclined well. In order to determine the true resistivity of the reservoirs, it is necessary to correct for the inclination of the formation. Firstly, the finite-element method was used to simulate the distribution of the electromagnetic field at the induction logging coils in the formation. Secondly, the induction logging resistivity at different inclination angles was determined by combining the total magnetic field strengths at the receiving coils, and a forward model of the resistivity was then established. Finally, the true resistivity of the formation was simulated by particle swarm optimization. The results showed that the resistivity increases as the dip angle increased. In this study, we used fitted forward and inversion models and the particle swarm optimization algorithm to correct the apparent resistivity of wells A and B in the Dabei Block in the Tarim Basin and thereby determine the resistivity of the formation. The effectiveness of the dip correction of the resistivity was confirmed by data from oil testing.

1. Introduction

Resistivity is the main parameter used to identify the properties of fluids in a reservoir. However, the dip, thickness and heterogeneity of the formation can cause distortions in the resistivity curve, which may lead to a misinterpretation of the nature of the reservoir fluids. Some studies have indicated that an essential feature of the resistivity is its anisotropy, in that it has directional variations in the formation (Gao et al., 2005; Shen et al., 2009). When the formation dip is low, the apparent resistivity (Ra) mainly corresponds to the horizontal component (R_h) of the resistivity. With an increase in the dip, the vertical component (R_v) of the resistivity is gradually becomes obvious (Xiao and Zhang, 1995; Deng et al., 2006; Fan et al., 2016). Shen et al. (2000) confirmed that the apparent resistivity increases with an increase in the formation dip.

With the development of computer science, the numerical simulation of resistivity has become an important method for solving the problem of resistivity anisotropy (Gao and Xie, 2000, 2003). Klein (1993) used the quantitative relationship between the borehole angle and the apparent resistivity to analyze the anisotropy of the induction logging. In order to improve the accuracy of the evaluation of formations, Hou et al. (2016) used multi-component induction logging to determine the formation dip, which was based on the anisotropic forward model of inclined formations (Epov et al., 2010). Gao et al. (2016) combined the lateral logging with three-dimensional finite-element numerical simulation to solve the problem of tendency and inclination and provided a theoretical basis for dip correction (Deng et al., 2012; Li et al., 2015). On this basis, Chen (2017) proposed a more effective finite-element method for simulating resistivity logging. Via forward modeling of the anisotropy of resistivity, the above-mentioned researchers discussed the influence of the formation dip on the resistivity, and established the forward theory of different formation dips. However, the inversion simulation of the effect of the dip on the resistivity and methods for the correction of this effect still lack effective research.

The study area is located in the Kelasu tectonic belt of the Kuqa foreland basin. The structure developed a set of salt layers in the Cretaceous system, which were subjected to strong tectonic compression, which therefore led to the occurrence of structural deformation between the upper and lower layers with the characteristics of a double-thrust structure. A nappe-type structure with a low thrust angle, a nappe-type structure with a steep dip angle, and an upward blockfault-type structure with a steep dip angle are developed in the upper salt layers. The lower salt layers are characterized by the development of superimposed

* Corresponding author.
E-mail address: zhaojun_70@126.com (J. Zhao).

https://doi.org/10.1016/j.petrol.2018.01.067
Received 6 August 2017; Received in revised form 14 January 2018; Accepted 30 January 2018
Available online 3 February 2018

thrust structures, as shown in Fig. 1. Strong tectonic compression increased the dip angle of the stratigraphic strata in the study area, and, as the dip angle of part of the strata is higher, the anisotropy of resistivity logging is more prominent, which causes difficulties in evaluating the fluid properties using the resistivity curve. In this study, the finite-element method was used to analyze the distribution characteristics of the electromagnetic field and potential gradient in induction logging at different dip angles. In combination with the particle swarm optimization (PSO) algorithm, this study established an inversion algorithm for resistivity. Via the processing of experimental data, the inversion algorithm generated a continuous dip correction of measured resistivity and provided an effective way of adjusting the dip correction of the resistivity.

2. Material and methods

This study considered the thickness of the target strata (h), the inclination angle (θ), the well diameter (D), and the position of the coil system used to log the structure of the strata. This study only considered the following parameters for the model: the resistivity of the target strata (R_t), the relative dielectric constant (ε_r), the differential permeability (μ_r), the resistivity of the surrounding rocks (R_s), and the resistivity of the mud in the wellbore (R_f). Fig. 2 shows four mesh models of the stratigraphy with different inclination angles.

In order to analyze the distributions of the electric field and the magnetic fields in the stratigraphic model, the finite-element method was used to solve the electric and magnetic field wave equations. When the coil size was compared with the coil spacing, the coil size was so small that it could be ignored. The transmitting coils could thus be considered to be equivalent to an oscillating magnetic dipole source in the induction logging. The vector wave equation for the magnetic field is shown in Equation (1):

$$\nabla \times \nabla \times \boldsymbol{H} - \omega^2 \mu \varepsilon_c H = \omega^2 \mu \varepsilon_c \boldsymbol{M_s} \tag{1}$$

where H is the magnetic field intensity, ω is the angular frequency, μ is the differential permeability, ε_c is the relative dielectric constant, and M_s is the magnetic flux density vector.

The wave equation should meet the two following boundary conditions in the formation model:

(1) The tangential component of the magnetic field should be continuous at the interface between formations.

$$\boldsymbol{n} \times (\boldsymbol{H}_1 - \boldsymbol{H}_2) = 0 \tag{2}$$

(2) The Dirichlet boundary condition should be met, whereby the flux at the model surface is zero.

$$\boldsymbol{H}|_{\infty} = 0 \tag{3}$$

This study used the finite-element method to solve the vector wave equation and then processed the distribution of the electromagnetic field generated by the transmitting coils to obtain the total magnetic field strength (H_R) at the receiving coils. Finally, the electromotive force induced in the receiving coils is obtained by the Faraday induction law:

$$V_i = -\frac{d\phi}{dt} = -i\omega N_n A_R \mu_0 \boldsymbol{H_R} \tag{4}$$

where V_i is the electromotive force induced in the ith receiving coil, Φ is the magnetic flux, N_n is the number of turns in the receiving coil, A_R is the area of the ith receiving coil, μ_0 is the permeability of free space, and H_R is the magnetic field intensity at the ith receiving coil.

For a compound coil system, the apparent resistivity values in the induction logs are obtained by the principle of superposition the electromagnetic field:

$$\sigma_a = \frac{\sum_{i=1}^{n} \sigma_i \sum_{j=1}^{m} \frac{N_{Ti} N_{Rj}}{L_{ij}}}{\sum_{i=1}^{n} \frac{N_{Ti} N_{Rj}}{L_{ij}}} \tag{5}$$

where σ_a is the apparent conductivity, σ_i is the apparent conductivity of the ith transmitting coil when the number of receiving coils is m, N_{Ti} is the number of turns in the ith transmitting coil, N_{Rj} is the number of turns in the jth receiving coil, L_{ij} is the distance from the ith transmitting coil to the jth receiving coil.

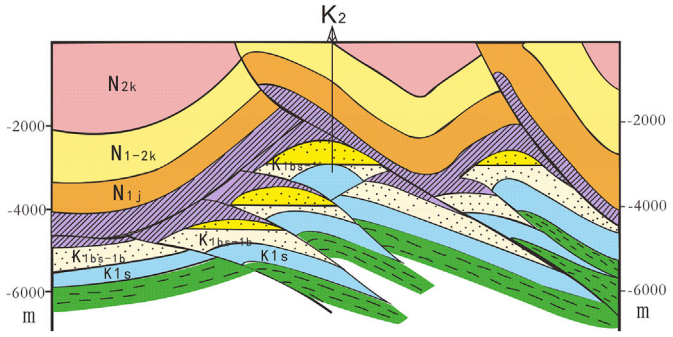

Fig. 1. Structure of the Dabei block.

3. Results

It was assumed that the formation was non-invasive and that the resistivity of the target strata was lower than of the surrounding rock. In Synthetic Example 1, the thickness of the target strata was 2 m, of which the resistivity was 5 Ω m, the relative dielectric constant (ε_r) was 10, and the differential permeability (μ_r) was 1.0. The resistivity of the surrounding rock was 40 Ω m, whereas the wellbore was filled with oil-based mud, of which the resistivity was 1000 Ω m. We determined the apparent resistivity for both deep and medium induction with changes in the measurement position, as shown in Fig. 3. Fig. 3a shows the apparent resistivity for deep induction, whereas Fig. 3b shows the apparent resistivity for medium induction in Synthetic Example 1.

In Synthetic Example 2, the initial conditions in the stratum model were changed so that the resistivity of the strata was 40 Ω m and the resistivity of the surrounding rock was 5 Ω m. We determined the apparent resistivity for deep and medium induction with changes in the measurement position, as shown in Fig. 4. Fig. 4a shows the apparent resistivity for deep induction, whereas Fig. 4b shows the apparent resistivity for medium induction in Synthetic Example 2.

Three conclusions can be drawn from the numerical simulation. First of all, at the same dip, there was a difference between the apparent resistivity values for deep and medium induction. The main reason is that the detecting depth for deep induction is greater than that for medium induction, and the corresponding measurements are thus affected by the upper and lower surrounding rocks to a greater extent. Secondly, as the dip angle increases, the apparent resistivity curves for deep and medium induction logging no longer have stratification capacity, and the curves develop increasingly obvious shoulders. Thirdly, the lower is the dip angle, the closer the induction logging resistivity is to the true resistivity of the formation.

The apparent resistivity is affected by factors such as dip, thickness and heterogeneity of the formation. In the case where only the influences of the dip and the resistivity anisotropy (λ) are considered, where λ is the cause of the difference between R_v and R_h, plots can be generated according to the abovementioned simulation results, as shown in Fig. 5. Fig. 5a shows that there was a good linear relationship between ln (Ra/Rh) and ln (Rv/Rh) at the same dip, and the slope increased with an increase in the dip. Fig. 5b shows that when the resistivity anisotropy coefficient was constant, there was a linear relationship between ln (Ra/Rh) and cos(θ), and the rate of change of ln (Ra/Rh) with cos(θ) increased as